Preprint
21st European Photovoltaic Solar Energy Conference and Exhibition, Dresden, Germany, 4.-8. September 2006

# ON LEAD AND CADMIUM FREE METALLIZATIONS FOR INDUSTRIAL SOLAR CELLS AND MODULES

Mario Bähr[1,*], Steve Kim[2], Sid Sridharan[2], Chandra Khadilkar[2], Jan Lossen[3], Stefan Dauwe[1,†]
[1]SolarZentrum Erfurt – CiS Institut für Mikrosensorik gGmbH, Konrad-Zuse Straße 14, 99099 Erfurt, Germany
[2]Ferro Ferro Corporation, 1395 Aspen Way, 92083 Vista (CA), USA
[3]ErSol Solar Energy AG, Wilhelm-Wolff Straße 23, 99099 Erfurt, Germany
[*]corresponding author: mbaehr@cismst.de, +49-361-663-1214

ABSTRACT: The reduction or even substitution of the heavy-metal content in an environmentally friendly Photovoltaic (PV) market is becoming an ever-increasing topic. This is to both a rising awareness of the PV industry to produce environmentally benign products as well as legislative restrictions. This paper deals mainly with efforts done in the development of lead- and cadmium-free metallization pastes for state-of-the-art screen-printing processes used for the metallization of industrial type silicon solar cells. New pastes for all metallization steps are available on either production or laboratory scale which meet the requirements for heavy-metal free applications in silicon solar cells and modules. All metal pastes used in typical industrial solar cells were replaced by lead- and cadmium-free ones and electrical performance, printability, contact and series resistances and adhesion of a soldered lead-free ribbon were investigated. Electrical performance and also adhesiveness of the lead-free metallization was found to be very similar to those of plumbiferous reference pastes.

Keywords: Screen-printed metallization, lead-free, module manufacturing

## 1 INTRODUCTION

The Restriction of the use of Certain Hazardous Substances (RoHS) is an EU directive for electric and electronic devices, regulating the maximum content of environmentally harmful substances including heavy-metals. RoHS came into force on 1st July 2006[1]. According to this restriction, a maximum content of 0.1 wt % lead (Pb) and 0.01 wt % cadmium (Cd) is allowed in homogeneous materials. Exceptions to these regulations exist only for hazardous substances for which either no substitutes exist or of which the substitutes are more dangerous than the substance itself. Besides heavy-metals, also flame retardants, such as polybrominated biphenyls (PBB) and polybrominated diphenyl ethers (PBDE) are affected.

Although these exceptions are applicable to solar cells and modules, there are already efforts to avoid Pb and Cd, since the “green” image of photovoltaics (PV) could otherwise be damaged. These exceptions are based on several aspects as will be discussed in the next paragraphs.

Hand in hand with the RoHS restriction goes the EU directive Waste on Electric and Electronical Equipment (WEEE)[2] which addresses the responsibility for a proper disposal to the manufacturers of electric and electronic devices. The PV is affect, since end devices which are powered by PV-modules are assigned to this directive.

The upcoming Registration, Evaluation and Authorization of Chemicals (REACH)[3] is an EU restriction, which will regulate the trade with chemicals produced and imported in EU territory. Companies trading more than 1 ton in volume of chemicals per year have to register, to evaluate and to authorize their products. The applicability to PV is given, since the law also dwells on the dangerousness of products that can be end up in the environment and so can come e.g. in the food chain and be harmful to humans. This law is under discussion, but is likely to be launched in 2007.

### 1.2 Heavy-metals in screen printed silicon solar cells

Standard industrial screen printed silicon solar cells contain heavy-metals from the metallization pastes in form of metal oxides called glass frits such as e.g. PbO-B2O3-SiO2. Besides the dissolution of the silicon nitride antireflection coating, which is accomplished by the glass frit in the front side paste, the frit generally improves the contact formation between the silicon and the metal in the pastes [4,5,6]. Contact formation is provided by a firing process at temperatures above 800 °C for at least some seconds. Schubert et al. found that between main compounds of metal inks, the silver and the glass frit, and the crystalline silicon a complex reaction system occurs: Within a redox reaction between metal oxide and silicon the crystalline silicon is partly dissolved. Further, the metal oxide serves as solvent for the silver. During cooling down after firing, the recrystallization of the molten compounds takes place, while the pure silver fills the partly dissolved silicon structures and thus a good contact is formed.

Pb- and Cd-free metallization pastes have already been commercialized for the rear side metallization [7,10]. In contrast, lead-free front side pastes are still in a laboratory stage and an industrial application is not known to the authors. But on a laboratory scale already some results have been published [8,9] or new front side metallization pastes which are free of heavy-metal were announced [10].

### 1.2 Heavy-metals in industrial type solar modules

Besides the heavy-metal content in the cells itself, also the ribbons used for the series connection are typically plated with a Pb-containing solder, such as Sn64Pb36 or Sn62Pb36Ag2. The existence of lead in an eutectic has the advantage of comparable low melting temperatures e.g. 183 °C for Sn63Pb37. In comparison, melting temperature for a lead-free solder such as Sn96.5Ag3.5 is 38 K higher. This higher thermal budget often leads to more thermally induced stress in the sample to be soldered and, in the worst case, the soldering procedure destroys the sample. But an adjusted

[†] now with: Schott Solar GmbH, Carl-Zeiss-Str.4, 63755 Alzenau, Germany

solder process together with an adapted flux leads to only a slightly higher risk of damage. With respect to this thermally induced stress, special attention has to be paid, when adapting a lead free soldering procedure to thin silicon solar cells. In this work lead-free solder connections were industrially processed and characterized.

## 2 EXPERIMENTAL

For the solar cells, 100 oriented mono crystalline silicon wafers of a size 156x156 mm² and a thickness of 200 µm were used. A standard industrial cell process was applied. This process consists of a KOH-damage and texture etch to remove about 10 µm silicon per side. Phosphorous diffusion was done using a $POCl_3$ source. This was followed by an edge isolation using a plasma etch in a microwave barrel reactor. After the removal of the phosphorus silicate glass in a HF-solution an amorphous silicon nitride layer ($SiN_X$:H) was deposited with a common low frequency plasma enhanced chemical vapor deposition system (PECVD). The screen printing of the front and rear was done with a conventional screen printer. The pastes used for the screen printing were mostly newly developed by Ferro Corp. This investigation especially focused on lead and cadmium free front side metallization pastes.

The experimental parameters are shown in Table I. Four groups of samples each having a different front side paste were processed. For group Ref, a lead- and cadmium-containing reference paste was used, while for group 36D, 40C or 40D, respectively, the newly developed lead and cadmium free pastes A386-36D, A386-40C or A386-40D were used. The new pastes differ in the type and contents of glass powder.

For all groups the same rear side aluminum paste CN53-101 was used, a standard lead-free product showing very good electrical performance and little bow values.

The rear side Ag/Al pastes for printing the rear busbars were again a lead containing reference paste FX33-130 (Group Ref) and a newly developed lead free pastes A386-20H and A386-20G (Groups 36D, 40C, 40D; see Table II). In former experiments performed at our institute, large scale tests of these three pastes showed an absolute identical behavior regarding electrical and mechanical performance. Hence, the differences in electrical performance found in the present experiments can only be attributed to the different front side metallization pastes.

After printing, the samples were co-fired in an IR belt furnace at already optimized firing temperatures and belt speed. The parameters used are also given in Table I. In order to measure the actual temperature on a metallised wafer, temperature profiles were measured using a data logger from Datapaq. During the measurement, the thermo couples were kept in close contact to the test wafer. In Figure 1 the temperature profile is shown for typical parameters used.

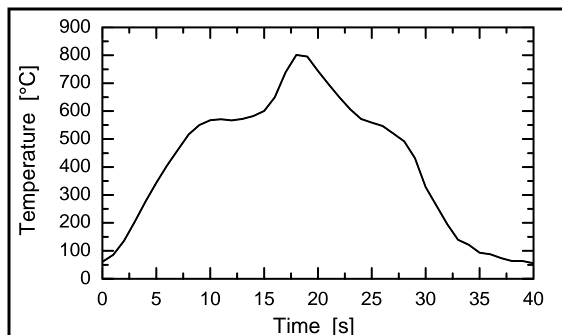


**Figure 1:** Typical temperature profile of a co-firing cycle used. The measurement was performed using a data logger from Datapaq.

**Table I:** Overview of parameters used in our study.

| | Group | | | |
|---|---|---|---|---|
| | *Ref* | *36D* | *40C* | *40D* |
| Front Ag | Ref | A386-36D | A386-40C | A386-40D |
| Lead | ~ 6 wt % | 0 | 0 | 0 |
| Rear Ag/Al | FX33-130 | A386-20H | A386-20G | A386-20H |
| Lead | 5 wt % | 0 | 0 | 0 |
| Rear Al | CN53-101 | | | |
| Lead | 0 | | | |
| Belt speed [m/min] | 3.0 | 3.3 | 3.3 | 3.3 |
| Temp. in spike zone [°C] | 885 | 940 | 945 | 910 |

## 3 TEST EQUIPMENT USED

### 3.1 Electrical performance

The electrical performance of the solar cells was measured using a standard solar simulator, featuring a flash lamp. The light IV curve was measured under standard test conditions (STC). Shunt resistance was determined by fitting the dark IV-curve for small voltages, while for the series resistance IV-curves under two different illumination levels (1000 and 500 W/m²) were used[11].

### 3.2 Printability / Finger geometry

Finger geometry was measured using a laser-based profilometer, µScan, from nanofocus. The laser head is positioned over the surface and measures height variations with a resolution of ± 0.5 µm, while the sample rests on a XY-table which is moved with a spatial resolution of 1 µm.

### 3.3 CoreScan

CoreScan measurements were used for determining the spatially resolved contact resistance of the front side contact structure. The measured potential is equivalent to a resistance and can be used for detecting problems in screen printing or firing since the signal can be

transferred into a contact resistance or resistivity. This method was introduced by van der Heide[12].

3.4 Contact resistance measurements

The contact resistance can be determined in detail using a screen printed structure different from the usual H-pattern[13].

3.5 Adhesion test

Adhesion is a very crucial parameter, since the junction between metallization and silicon as well as between metallization and solder ribbon has to endure thermally induced mechanical stress in the solar module for long times.

To make sure that a lead and cadmium free solar module can be manufactured, the used ribbon was a lead-free SnAg3.5 alloy, provided by Schlenk, with the cross section dimensions 2.1 x 0.20 mm². The flux used was Interflux 2005 M. In order to guarantee the industrial applicability the soldering was performed using an automated tabber-stringer. This tabber-stringer uses an infrared heating element, which heats up the fluxed ribbon and the cell in the busbar region. Further, the stringed cells were divided into single cells on which the pull up tests were performed.

A setup commonly used for characterization of soldered connection is shown Figure 2. The soldered ribbon is pulled from the solar cell. The strength of the measured force is a very good value for deciding whether the soldered connection is sufficient or not. In this work, a measuring system from GP Solar (Stab-test) was used, where the cell is fixed at an angle of 45° to the pull direction. The sample holder is mounted and the load cell is moving upwards. The measured force contains both, the force between ribbon and metallization as well as the adhesiveness of the metallization to the silicon. The force needed to bend the ribbon is neglected, since the same ribbon was used for all samples.

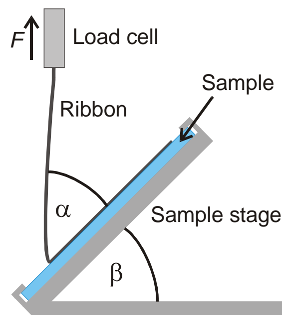


**Figure 2:** Setup for pull up measurements. The stage where the sample is fixed is arranged under an angle $\alpha = \beta = 45°$.

## 4 RESULTS

4.1 Electrical results

In Figure 3 the electrical parameters of the samples investigated are shown. Average values and standard deviations are shown as function of the front side paste used. Please note that only the groups 36D and 40D are printed with the same rear side Ag/Al paste. For the other groups different metallization pastes were used (see also Table I).

The number of cells used is in the range of 13 to 24. Since mono crystalline silicon was used, the variations in material quality can be neglected and different numbers of cells per group were tolerated.

It can be seen, that short-circuit current densities ($J_{SC}$) for the groups Ref and 36D are on a similar level at about 35.0 mA/cm² with a standard deviation of about 0.10 to 0.15 mA/cm². Groups 40C and 40D show smaller $J_{SC}$ values of 34.7 and 34.8 mA/cm², respectively. These smaller values can be attributed to wider fingers due to a spreading of the printed fingers (see paragraph 4.2).

Open circuit voltages ($V_{OC}$) for the lead-free pastes ranges from 612 to 613 mV, that is about 4–5 mV higher compared to the 608 mV of group Ref. This increased $V_{OC}$ can be attributed to a better rear surface passivation.

Significant differences were observed in fill factor ($FF$). Very high $FF$s of about 77.4 ± 0,4 % were measured for the group Ref, whereas $FF$ for group 36D, is only 72.1 ± 1.0 %, for group 40C about 76.2 ± 0.3 % and for group 70D about 76.5 ± 0.3 %. This can be attributed to the different series resistances ($R_{SER}$) which are about 0.7 Ωcm² for the reference group but higher for the lead-free groups: 1.9 Ωcm² (36D), 0.9 Ωcm² (40C) and 1.0 Ωcm² (40D). Standard deviations are in the range of 0.08 to 0.18 Ωcm². Contact resistance measurements clarify these results (sections 4.4 and 4.5). Although differences in shunt resistance ($R_{SHUNT}$) were observed, the measured values of well above 5 kΩcm² will not effect the fill factor.

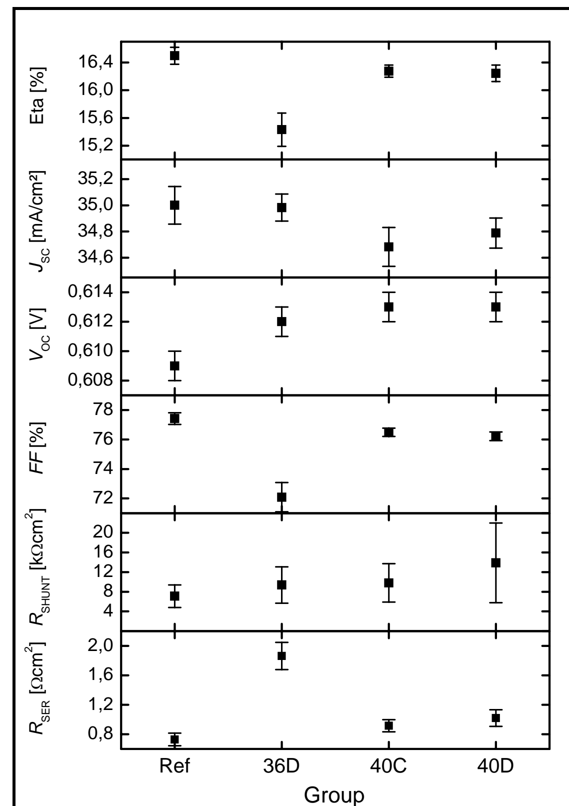


**Figure 3:** Electrical results of the samples tested. Averages and standard deviations of at least 13 cells for each variation are shown.

The highest efficiencies (Eta) were observed for the reference group with about 16.5 ± 0.1 %. For the lead-free groups Etas of 15.4 ± 0.2 %, 16.3 ± 0.1 % and 16.2 ± 0.1 % were measured for groups 36D, 40C and 40D, respectively. These differences can be explained by means of slightly lower $J_{sc}$ and FF values in case of 40C and 40D and much lower FF values in case of 36D.

Obviously, similar efficiencies can be obtained using lead- and cadmium-free metallization pastes instead of lead containing ones.

4.2 Finger geometry

Results of the finger-geometry measurements are presented in Table II. The finger widths were confirmed by visual inspection using an optical microscope.

For the finger width smaller values of about 136 and 128 µm for the groups Ref and 36D were measured, compared to the groups 40C and 40D with 162 and 170 µm. Due to the spreading of the pastes of groups 40C and 40D, the fingers were leveled off and the heights decreased to values of about 13 µm (40C) and 18 µm (40D). High cross section areas were measured all these samples. Paste 36D suffered from a non-optimal viscosity, because the fingers processed were narrow as well as plane and so only small cross sections were obtained.→→

**Table II:** Finger geometry in terms of foot width, height, cross section area and aspect ratio for 3 measurements from one sample per group which shows a typical electrical performance.

| | Ref | 36D | 40C | 40D |
|---|---|---|---|---|
| width [µm] | 136 | 128 | 162 | 170 |
| height [µm] | 22 | 11 | 13 | 18 |
| cross section area [µm²] | 1654 | 929 | 1449 | 2056 |
| aspect ratio | 0,16 | 0,09 | 0,08 | 0,11 |

4.3 CoreScan

Two CoreScan mappings of the local potential of two different samples are shown in Figure 4. Note that both graphs are scaled identically. Out of several measurements one typical sample from group 36D and one from group 40C are presented. The higher potential observed in Figure 4a shows fundamental problems of the front side metallization. The right samples suffers only from 2 finger constrictions due to an inhomogeneous printing.

To get quantitative information, all data in y-direction were averaged. Different averaged potentials in one chart allow for a good comparison, provided that the distribution on the samples is quite homogeneous. The following Figure 5 shows four typical curves of one sample of each group.

The curves presented show similar results as in contact resistance and line resistance for groups Ref, 40C and 40D: Differences between minima (corresponds to metallization finger) and maxima (in-between two neighboring met. fingers) are nearly equal for these

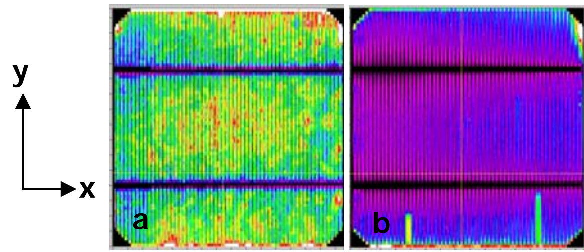


**Figure 4:** CoreScan topographies with same scaling (0-30 mV) of two different cells: a) Group 36D (*FF* = 73.2 %, $R_{SER}$ = 1.72 Ωcm², $U_{average}$ = 13.6 mV), b) Group 40C (*FF* = 76.1 %, $R_{SER}$ = 1.06 Ωcm², $U_{average}$ = 5.0 mV).

groups. The line resistance of a metallization is equal to the minimum values at the finger positions. As can be seen, the measured potentials are on a low level of about 0.5 mV for these three groups.

For group 36D large deviations compared to the other groups were found: The contact resistance as well as the line resistance are significantly increased. So, the increased series resistance and lower fill factor can clearly be attributed to the increased contact resistance and line resistance. Since the cross section is significantly lower than others, this can provoke higher line resistances as well.

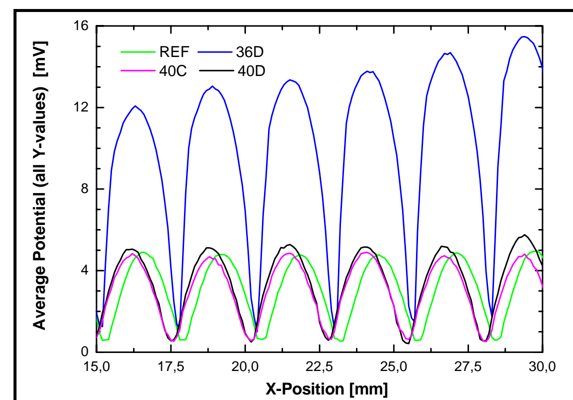


**Figure 5:** Averaged CoreScan potentials of CoreScan measurements from one typical sample of each group.

4.4 Contact resistance

Contact resistances were measured on up to 5 samples per group. Results are presented in Table I. The measured contact resistances show strong variations. Contact resistance measurements are going hand in hand with the results of the corescan measurements: For groups Ref, 40C and 40D significantly lower mean contact resistances were measured, as compared 36D, for which nearly doubled resistances were measured. Due to strong variations in the single values the standard deviations are in the range of 20 %. Not the very low contact resistances which were found for paste A386-40C.

**Table III:** Contact resistances measured using Meier-Schroder test structures.

| Contact resistance [Ω] | Ref | 36D | 40C | 40D |
|---|---|---|---|---|
| Average | 0,84 | 1,55 | 0,68 | 0,94 |
| Standard deviations | 0,23 | 0,33 | 0,23 | 0,20 |

4.5 Pull up forces

In Figure 6 typical measurements of the pull up force vs. the pull up distance are shown. At least 4 samples per group were measured, but because of the complexity of all values only one typical curve is shown. As can be seen, the measured forces are not at the same level for a certain sample. This behavior was found for nearly all samples measured. The inhomogenities occur due to inhomogenities in the wetting of the flux, in solder temperature, and in the force which is applied when pressing down the ribbon during soldering. Hence, these observations can be considered as typical.

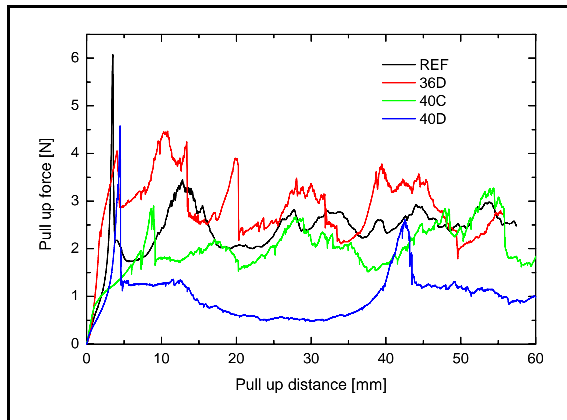


**Figure 6:** Measured pull up forces for the front side metallization vs. pull up distance for one typical sample of each group. Lead-free ribbons were soldered to the front-side metallization using an automated tabber stringer system. Between 15 and 40 mm the ribbon was not soldered to the metallization of the sample from group 40D.

In Table IV the statistics on all 4 samples measured per group are given. The curves of Figure 6 correspond well to the results of Table IV: Highest median values of about 1.7 N were measured for the samples of group Ref and 36D. A lower value of about 1.5 N was found for the sample of group 40C and even lower values of about 0.5 N were measured for the sample of group 40D.

These results show that, using heavy-metal-free front side pastes such as A386-36D or -40C instead of a heavy-metal-containing paste, also a sufficient adhesion strength can be obtained.

**Table IV:** Statistics on the pull up test. For 4 measurements per group the measured forces were analyzed in terms of median, average, standard deviation and maximum force.

| Pull up forces [N] | Ref | 36D | 40C | 40D |
|---|---|---|---|---|
| Median | 1,7 | 1,7 | 1,5 | 0,7 |
| Average | 1,7 | 1,9 | 1,4 | 0,8 |
| Std. Dev. | 0,7 | 0,8 | 0,6 | 0,5 |
| Max | 6,1 | 4,5 | 3,3 | 4,6 |

## 5 CONCLUSIONS

In this work, newly developed lead- and cadmium-free metallization pastes for screen printing applications were investigated. The work was focused especially on front side pastes. The obtained electrical results of the pastes A386-40C and A386-40D are virtually the same as for the lead-containing reference paste. The mean efficiencies of processed monocrystalline wafers were about 16.5 % for the reference and 16.3 and 16.2 % for both heavy-metal free pastes. Smaller fill factors due to higher series resistances and smaller $J_{SC}$ values are held responsible for these lower efficiencies. However, the lower $J_{SC}$ values can fully be attributed to a spreading of the metallization structures. Contact resistances measurements showed similar results for both heavy-metal-containing as well as heavy-metal-free pastes. The reasons for the increased series resistance remains obscure at present.

Also, the crucial parameter adhesiveness of a soldered connection was measured. Ribbons with a lead-free solder were soldered in an automated system onto the solar cells and peeling measurements were performed. The lead-free pastes showed very good adhesivenesses: Pull up forces in the range between 1 and 3 N were measured for all pastes tested.

The very good electrical performance and adhesiveness of lead-free solder connections ensure the applicability of the tested front-side metallization pastes, which are free of heavy-metal.

## 6 ACKNOWLEDGMENTS

The authors whish to thank F. Jaworowski from ASS GmbH, Erfurt, Germany, for performing the soldering. Special thanks go to S. Nieland for advice in soldering and M. Reichardt for help in characterization. The financial support by the Thüringer Aufbaubank (TAB) and the German Bundesministerium für Wirtschaft und Arbeit (BMWA) is gratefully acknowledged.

## 7 REFERENCES

[1] European directive RoHS : 2002/95/EC
[2] European directive WEEE : 2002/96/EC
[3] European directive REACH : Proposal 52003PC0644(01)
[4] Schubert et al.: “Physical understanding of printed thick film from contacts of crystalline Si Solar cells: Review of existing models and recent developments”, Proceedings 14th PVSEC, Bangkok, 2004, 441-442
[5] Baliff et al.: “Silver thick-film contacts on highly doped n-type Si emitters: structural and electronical properties of the interface”, Appl. Phys Lett. 82, 2003, pp.1878-1880
[6] Schubert et al.: “Silver thick film contact formation on lowly doped phosphorous emitters”, Proceedings 20th EPVSEC, 2005 Barcelona, pp. 934-937
[7] Kim et al. “Towards development of lead-free thick film inks for crystalline silicon solar cells”, Proceedings 20th EPVSEC, 2005 Barcelona, pp. 834-837

[8] Hoornstra et al.: "-free metallization paste for crystalline silicon solar cells : from model to results", Proceedings 31st IEEE PVSEC, Orlando 2005, pp. 651-654

[9] Carroll et al.: "Advances in PV metallization technology", Proceedings 20th EPVSEC, Barcelona 2005, pp.906-909

[10] Photon International, magazine, 2006-07, pp. 96 et sqq.

[11] IEC Standard IEC-891

[12] Heide, A.S.H. van der, et al.: „Error diagnosis and optimisation of c-Si solar cell processing using contact resistances determined with the Corescanner", Solar Energy materials and solar cells 74, 2002, 43-50

[13] Schroder: "Semiconductor material and device characterization", 2nd edition 1998, pp. 138 et sqq.